Available online at www.sciencedirect.com

SciVerse ScienceDirect

Ceramics International 38 (2012) 2269–2276

CERAMICS INTERNATIONAL

www.elsevier.com/locate/ceramint

Phase evolution and thermal behaviors of the solid-state reaction between $SrCO_3$ and Al_2O_3 to form $SrAl_2O_4$ under air and CO_2-air atmospheres

Yu-Lun Chang [a], Hsing-I Hsiang [a,*], Ming-Tsai Liang [b], Fu-Su Yen [a]

[a] *Particulate Materials Research Center, Department of Resources Engineering, National Cheng Kung University, No.1, University Road, 70101 Tainan, Taiwan, ROC*

[b] *Department of Chemical Engineering, I-Shou University, Kaoshiung 840, Taiwan, ROC*

Received 7 October 2011; received in revised form 26 October 2011; accepted 27 October 2011
Available online 4 November 2011

Abstract

The solid-state reactions between $SrCO_3$ and Al_2O_3 forming $SrAl_2O_4$ under air and CO_2-air atmospheres were investigated. The solid-state reaction between $SrCO_3$ and Al_2O_3 under a CO_2 atmosphere can be separated into multiple reaction stages. The first stage is attributed to the formation of $SrAl_2O_4$ resulting from the reaction between $SrCO_3$ and Al_2O_3. The diffusion of Al_2O_3 through the product layer then takes place to continue the reaction. At a higher temperature, the $Sr_3Al_2O_6$ formation reaction occurs due to the chemical reaction between $SrCO_3$ and $SrAl_2O_4$. The $SrCO_3$ is thermally finally decomposed. The resulting SrO may diffuse rapidly through the product layer, producing pure $SrAl_2O_4$ formation via a complicated diffusion process at a much higher temperature. These reaction stages occur at very close temperatures under an air atmosphere, leading to a complex reaction between the solids in air.

Keywords: A. Calcination; A. Powders: solid state reaction; B. Defects; C. Diffusion; $SrAl_2O_4$

1. Introduction

Strontium mono-aluminate, $SrAl_2O_4$, is a promising host material for luminescent appliances. Various optical properties can be achieved by doping rare earth ions or transition metal ions within the structure [1–3]. $SrAl_2O_4$ is a thermodynamically stable compound that possesses the stuffed tridymite structure. This structure is built by AlO_4^{5-} tetrahedra and Sr^{2+} ions stuffed into the framework interstices. It has two crystalline phases, monoclinic and hexagonal, with a reversible transformation temperature of about 650 °C. $SrAl_2O_4$ can be synthesized using many methods, such as the combustion method [4], spray pyrolysis [5], sol–gel route [6], Pechini process [7], and solid-state process [8,9]. Because of its' low manufacturing costs and convenient operation, $SrAl_2O_4$ is usually prepared using the conventional solid-state reaction.

The solid-state synthesis of $SrAl_2O_4$ is usually carried out using $SrCO_3$ and Al_2O_3 as the raw materials. The solid-state reaction between $SrCO_3$ and Al_2O_3 to form $SrAl_2O_4$ was investigated by Zaki et al. [10]. Their kinetic data indicates that the reaction is controlled by the diffusion model and SrO diffusion through the product layer is suggested. Camby and Thomas investigated the interfacial reaction between $BaCO_3$ and Al_2O_3 using diffusion couples [11] and observed that $BaAl_2O_4$ was the only product resulting at 900 °C. After calcination for 5 days, $Ba_3Al_2O_6$ was further observed located at the interface between $BaCO_3$ and $BaAl_2O_4$. Another product, $BaAl_{12}O_{19}$, was also formed at the interface between $BaAl_2O_4$ and Al_2O_3. They considered that the $Ba_3Al_2O_6$ nucleation was attributed to the dissolution of interstitial Ba^{2+} within the $BaAl_2O_4$ structure, and could grow as long as the reaction persisted. The formation of $BaAl_{12}O_{19}$ was not elucidated. However, a composition with a large departure from stoichiometry in the $BaAl_{12}O_{19}$ layer was observed. Moreover, Gulgun et al. [12] used a chemical method to synthesize $CaAl_2O_4$ and observed that the activation energy in $CaAl_2O_4$ formation is comparable to that of Ca^{2+} diffusion in CaO, but far from the Al^{3+} diffusion in Al_2O_3. Therefore, the nucleation mechanism of $CaAl_2O_4$ is controlled by the diffusion of Ca^{2+} and the growth of $CaAl_2O_4$ is further dominated by Ca^{2+}

* Corresponding author. Tel.: +886 6 2757575x62821; fax: +886 6 2380421.
E-mail address: hsingi@mail.ncku.edu.tw (H.-I. Hsiang).

0272-8842/$36.00
doi:10.1016/j.ceramint.2011.10.077

diffusing through the product layer toward Al_2O_3. Thus, it can be concluded that the solid-state reaction to form stuffed tridymite, MAl_2O_4, M = Ca, Sr, or Ba, is usually dominated by the diffusion of M^{2+} ions.

In our previous study, Al^{3+} ions diffused was observed in the reaction system for $SrAl_2O_4$ formation [13]. The high temperature hexagonal $SrCO_3$ and hexagonal $SrAl_2O_4$ phases stabilized at room temperature are suggested to incorporate the excess Al_2O_3 into the $SrCO_3$ and $SrAl_2O_4$ lattices resulting from Al^{3+} ion diffusion. This indicates that the solid-state reaction between $SrCO_3$ and Al_2O_3 is a complicated reaction mechanism rather than a simple process. In order to understand the reaction mechanism more completely, the solid-state reaction between $SrCO_3$ and Al_2O_3 was carried out under air and CO_2 atmospheres. The phase evolution and reaction mechanisms were carefully investigated using DTA/TG, XRD and TEM to propose a possible reaction mechanism.

2. Experimental

$SrCO_3$ (Aldrich, 99.99%) and α-Al_2O_3 (Alfa Aesar, 99.9%) were mixed at a stoichiometic ratio by magnetically stirring the aqueous solution for 4 h. The pH value of the aqueous solution was adjusted to 9.5 by adding NH_4OH. After mixing, the obtained mixtures were dried and calcined at different temperatures. The crystalline phases of the samples were determined using X-ray diffractometry (Siemens, D5000, Karlsruhe, Germany) with Cu-K_α radiation. TEM (Jeol, JEM-3010, Tokyo, Japan) was used to observe the crystallite size and morphology. The diffraction patterns of the crystalline species were obtained using TEM with a camera constant of 80 cm. Semi-quantitative determination of the element content was detected using EDS (Noran, Voyager 1000, Waltham, MA) attached to the TEM. The DTA/TG analysis was performed using a thermal analysis instrument (Netzsch STA, 409 PC, Burlington, MA) under 40 ml/min flow rate of carrier gas.

3. Results and discussion

3.1. The phase evolution

Fig. 1 shows XRD patterns of the mixture calcined at 980 °C under atmospheres with different CO_2 concentrations. The monoclinic $SrAl_2O_4$ and the $Sr_3Al_2O_6$ were observed in the sample calcined in air. As the CO_2 concentration was increased to 3 vol% CO_2, hexagonal $SrCO_3$ and hexagonal $SrAl_2O_4$ were formed while $Sr_3Al_2O_6$ started to appear. By increasing the CO_2 concentration, the amount of $Sr_3Al_2O_6$ formation gradually decreased. Above 10 vol% CO_2, only hexagonal $SrCO_3$ and hexagonal $SrAl_2O_4$ were observed. This indicates that the phase evolution between $SrCO_3$ and Al_2O_3 is significantly influenced by the CO_2 partial pressure.

In the previous study [13], stabilized hexagonal $SrCO_3$ and hexagonal $SrAl_2O_4$ were also observed in the sample calcined using a covered crucible. It is supposed that the CO_2 gas accumulation in the covered crucible provided a CO_2 atmosphere. The stabilizations of hexagonal $SrCO_3$ and hexagonal

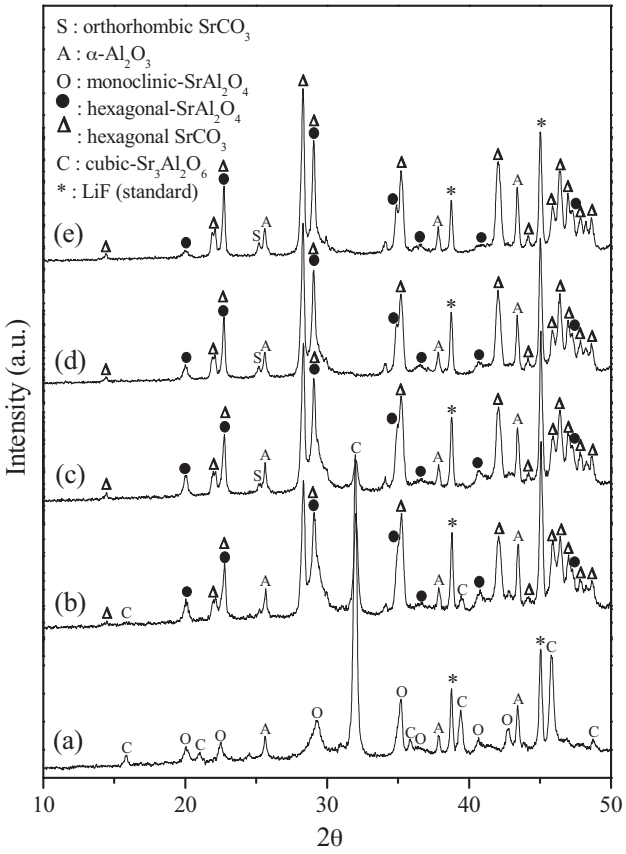

Fig. 1. XRD patterns of the $SrCO_3$ and Al_2O_3 mixture calcined at 980 °C without soaking under atmospheres with different CO_2 concentration, (a) in air, (b) 3 vol%, (c) 5 vol%, (d) 10 vol%, and (e) 20 vol%.

$SrAl_2O_4$ were attributed to Al_2O_3 incorporation. The incorporation of excess Al_2O_3 into the $SrAl_2O_4$ structure is suggested to increase the oxygen vacancy concentration. The resulting oxygen vacancy can stabilize the high temperature hexagonal $SrAl_2O_4$ at room temperatures [14,15]. The increase in crystal volume due to the transformation from orthorhombic to hexagonal $SrCO_3$ may introduce Al_2O_3 diffusion into the interstices, which may raise the internal strain energy and suppress the reversible phase transformation of $SrCO_3$. Therefore, the high temperature hexagonal $SrCO_3$ phase can be retained at room temperature. A metastable $SrCO_3$ phase was also obtained by quenching from the phase transition temperature using the admixture of a few mol% of $BaSO_4$. The incorporation of SO_4^{2-} in the host structure was triggered by the $SrCO_3$ phase transformation [16]. This observation is consistent with the fact that Al^{3+} ion diffusion into the $SrCO_3$ lattice is promoted by the $SrCO_3$ transformation from the orthorhombic into the hexagonal.

Lander investigated the crystal structure of $SrCO_3$ at 920 °C and observed that the lattice parameters of the hexagonal $SrCO_3$ crystal were $a = 5.092$ Å and $c = 9.53$ Å and the most intense X-ray diffraction occurred at $2\theta = 27.66$ [17]. However, the most intense XRD peak in the stabilized hexagonal $SrCO_3$ occurred at $2\theta = 28.34$ in this study. This is probably due to the crystal distortion in the hexagonal crystal structure. The Miller indices of the diffraction peaks for the resulting hexagonal

Table 1
Miller indices of the diffraction peaks for the resulting hexagonal $SrCO_3$ based on the XRD result.

2θ	d spacing (1/Å)	$h\,k\,l$
14.478	6.138	0 0 2
21.898	4.055	0 0 3
22.097	4.018	1 0 0
22.728	3.909	1 0 1
28.343	3.148	1 0 2
29.953	2.981	0 0 4
35.212	2.547	1 0 3
42.082	2.146	1 1 0

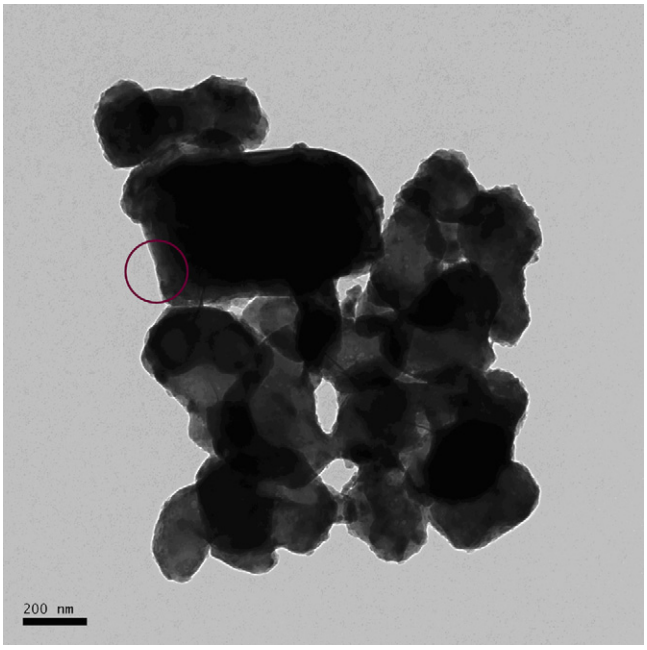

Fig. 2. TEM photograph of the mixture calcined at 980 °C under 10 vol% CO_2 atmosphere.

$SrCO_3$ based on the XRD result are shown in Table 1. The lattice parameters of this stabilized structure are suggested to be a = 3.99 Å and c = 10.49 Å. Fig. 2 shows a TEM photograph of the $SrCO_3$ and Al_2O_3 mixture calcined at 980 °C under 10 vol% CO_2 atmosphere. The loosely packed particles with size around 200–400 nm are ascribed to Al_2O_3 using EDS confirmation. The selected area diffraction pattern and the EDS result for a larger particle with a particle size around 800 nm are shown in Fig. 3. The stabilized hexagonal $SrCO_3$ particles can be assigned based on the TEM diffraction pattern, which coincides well with the proposed diffraction index. Moreover, additional Al content was also observed in this area, indicating the existence of Al_2O_3 within the structure.

3.2. The thermal behaviors

Fig. 4 shows DTA/TG curves of the $SrCO_3$ and Al_2O_3 mixture in air. About four endothermic peaks from the DTA curve are observed starting at 800 °C, 890 °C, 930 °C, and 980 °C. The sharpest peak at 930 °C is ascribed to the $SrCO_3$ phase transformation from orthorhombic to hexagonal [17]. The other peaks, which correspond to a multiple step weight loss in the same temperature range, can be attributed to the chemical reaction involving $SrCO_3$ of the samples. The total weight loss levels off at around 1020 °C.

Thermal analyses of the $SrCO_3$ and Al_2O_3 mixtures were performed to investigate the possible solid state. Fig. 5 shows the DTG curves of the $SrCO_3$ and Al_2O_3 mixtures, $SrCO_3$ and $SrAl_2O_4$, and pure $SrCO_3$ in air. Three indistinct weight loss stages in the $SrCO_3$ and Al_2O_3 mixture take place in 800–1020 °C temperature range, which coincide well with the multiple peaks in the DTA investigation. On the other hand, the weight loss in the $SrCO_3$ and $SrAl_2O_4$ mixture and pure $SrCO_3$ both reveal a single peak at a similar temperature range to that of the $SrCO_3$ and Al_2O_3 mixture, but the onset temperature of

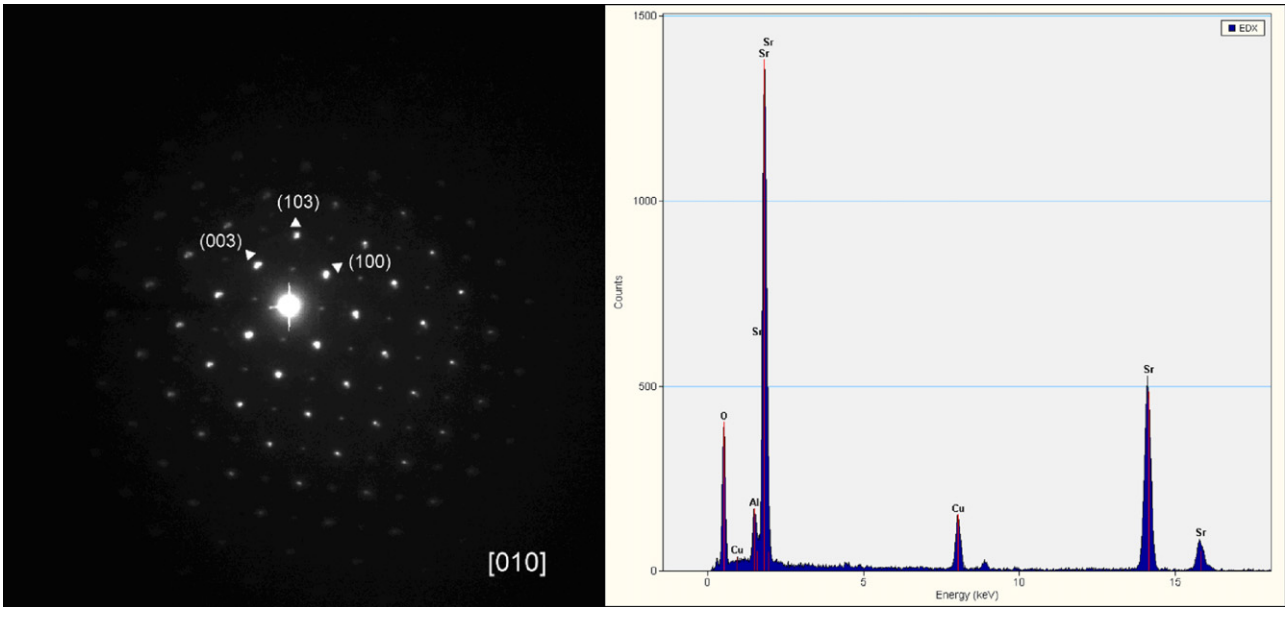

Fig. 3. Diffraction pattern and EDS result of the selected area in the TEM photograph.

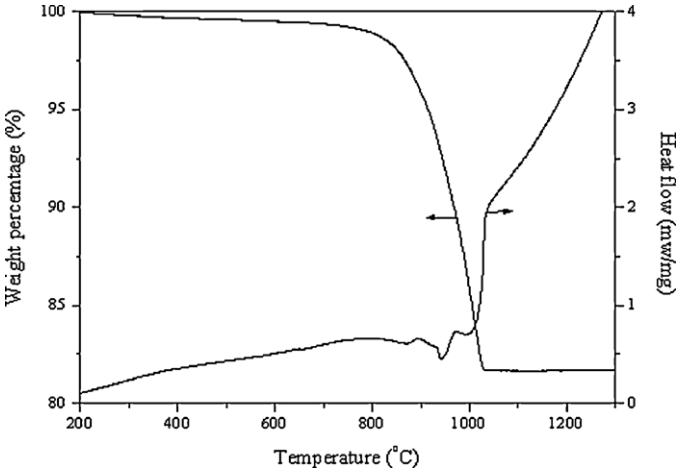

Fig. 4. DTA/TG curves of the $SrCO_3$ and Al_2O_3 mixture in air.

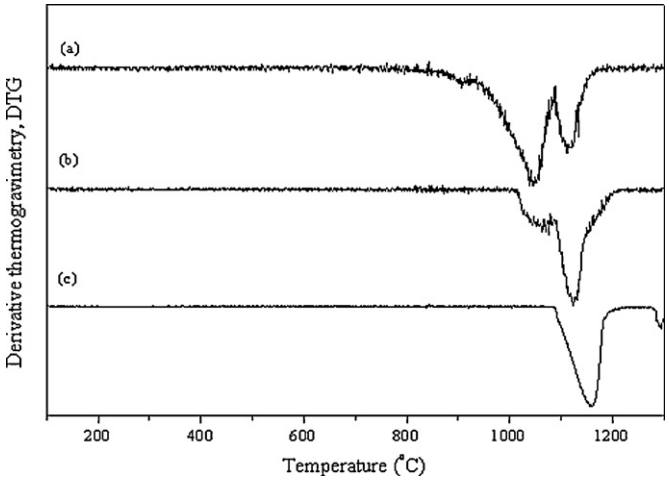

Fig. 6. DTG curves of the mixture under 10 vol% CO_2 atmosphere, (a) $SrCO_3 + Al_2O_3$, (b) $2SrCO_3 + SrAl_2O_4$, and (c) pure $SrCO_3$.

the $SrCO_3$ and $SrAl_2O_4$ mixture was slightly higher than that of pure $SrCO_3$. This indicates that the temperatures for the different reaction stages for each sample are overlapped and the complicated reactions between the reactants are still difficult to resolve. The DTG curves changed significantly when the atmosphere became 10 vol% CO_2 (Fig. 6). Three distinguishable stages of weight loss for the $SrCO_3$ and Al_2O_3 mixture under 10 vol% CO_2 atmosphere were observed. The first stage starts at near 850 °C, which is close to that of the reaction in air. The second stage starts at a temperature near 900 °C, and the third weight loss occurs at around 1100 °C. The $SrCO_3$ and $SrAl_2O_4$ mixture shows two stages of weight loss. The first stage starts at a temperature around 1000 °C and another occurs near 1100 °C. For the pure $SrCO_3$, an obvious weight loss peak starts at around 1100 °C, followed by a trace weight loss near 1300 °C.

In the $SrCO_3$ and Al_2O_3 solid-state reaction under 10 vol% CO_2 atmosphere, the weight loss stages are shifted toward higher temperatures and become distinguishable compared to that under an air atmosphere. This shows that these reactions are sensitive to CO_2 partial pressure. From the thermodynamic aspect, the thermal decomposition temperature of $SrCO_3$ in air alone (Eq. (1)) must be greater than 1000 K [18]. Nevertheless, the thermal decomposition of $SrCO_3$ can be promoted by a subsequent reaction with a lower free energy, such as followed by $SrO + Al_2O_3 \rightarrow SrAl_2O_4$ at around 690 K, and followed by $2SrO + SrAl_2O_4 \rightarrow Sr_3Al_2O_6$ at around 850 K (Fig. 7). These combination reactions can be referred to as direct reactions to form $SrAl_2O_4$ (Eq. (2)) and $Sr_3Al_2O_6$ (Eq. (3)), respectively. By increasing the CO_2 concentration to 10 vol%, the $SrCO_3$ decomposition temperature is raised from 1000 K to near 1280 K, thereby suggesting an increase in the reaction temperature for the related combination reactions.

$$SrCO_3 \rightarrow SrO + CO_2 \quad (1)$$

$$SrCO_3 + Al_2O_3 \rightarrow SrAl_2O_4 + CO_2 \quad (2)$$

$$2SrCO_3 + SrAl_2O_4 \rightarrow Sr_3Al_2O_6 + 2CO_2 \quad (3)$$

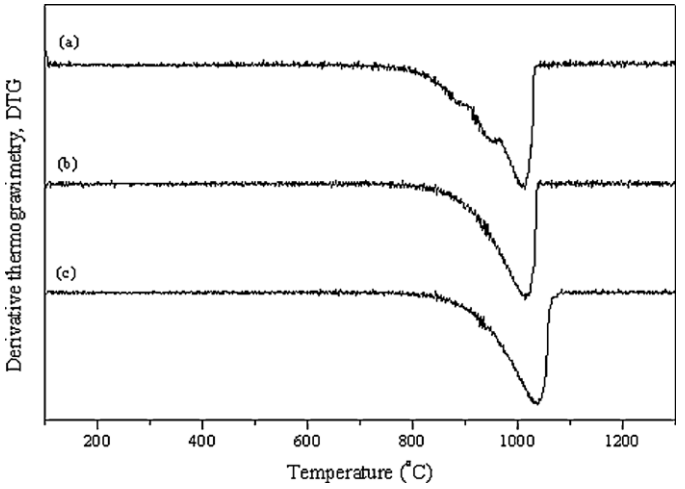

Fig. 5. DTG curves of the mixture in air, (a) $SrCO_3 + Al_2O_3$, (b) $2SrCO_3 + SrAl_2O_4$, and (c) pure $SrCO_3$.

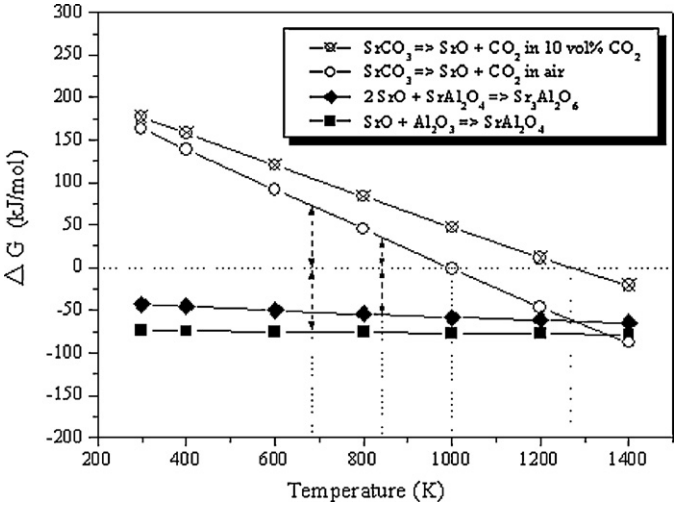

Fig. 7. Calculated Gibb's free energies of the possible reactions in the solid-state reaction system.

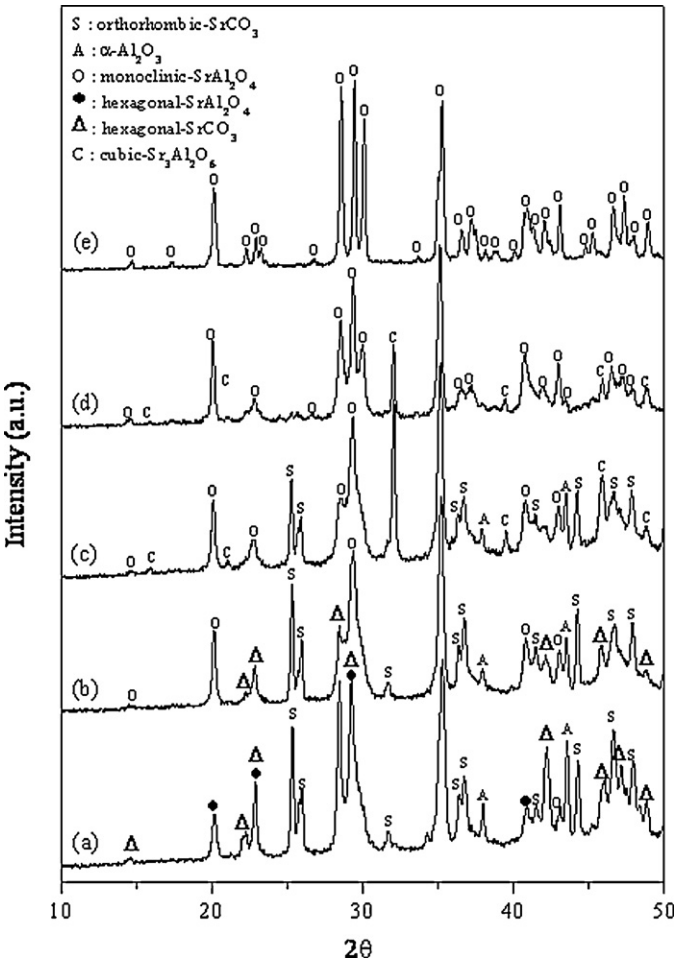

Fig. 8. XRD patterns of the $SrCO_3$ and Al_2O_3 mixture calcined at different temperatures under 10 vol% CO_2 atmosphere, (a) 950 °C, without soaking, (b) 950 °C, 4 h, (c) 1030 °C, without soaking, (d) 1200 °C, without soaking, and (e) 1300 °C, 2 h.

3.3. The reaction mechanism

Camby reported the formation of $BaAl_2O_4$ in the earliest reaction stage between $BaCO_3$ and Al_2O_3 [11]. The thermodynamic results also indicate the reaction occurring at the lowest reaction temperature for the reaction between $SrCO_3$ and Al_2O_3 is due to the reaction to form $SrAl_2O_4$ (Eq. (2)). Therefore, the first weight loss stages for the solid-state reaction between $SrCO_3$ and Al_2O_3 (at 800 °C in air, and at 850 °C under 10 vol% CO_2 atmosphere) can be attributed to the formation of $SrAl_2O_4$ according to Eq. (2). Because of the lower dissociation energy of SrO than Al_2O_3, the prevailing diffusion of Sr^{2+} ions for the formation of $SrAl_2O_4$ [10] is suggested in this stage.

The second stage of the $SrCO_3$ and Al_2O_3 mixture under 10 vol% CO_2 atmosphere, consists of two kinds of reactions. The weight loss occurs at 1030–1100 °C, which corresponds to the first weight loss stage for the $SrCO_3$ and $SrAl_2O_4$ mixture (Fig. 6). This can be reasonably attributed to the interfacial reaction between $SrCO_3$ and $SrAl_2O_4$ for the formation of $Sr_3Al_2O_6$ (Eq. (3)). Furthermore, a trace reaction is observed in the narrow 900–1030 °C temperature range, which is lower than that for the $Sr_3Al_2O_6$ formation reaction from $SrCO_3$ and $SrAl_2O_4$. Fig. 8 shows the XRD results for samples calcined at different conditions under 10 vol% CO_2 atmosphere, indicating that only hexagonal $SrCO_3$ and hexagonal $SrAl_2O_4$ occurred at 950 °C. By increasing the holding time to 4 h, a small amount of hexagonal $SrCO_3$ still remained and no intermediate phase, $Sr_3Al_2O_6$, was observed. This suggests that the reaction in the temperature interval resulted mainly in $SrAl_2O_4$ formation. After the first reaction stage, the unreacted $SrCO_3$ and Al_2O_3 were separated by $SrAl_2O_4$ grains, which suppressed the decomposition of unreacted $SrCO_3$ due to the decomposition temperature of pure $SrCO_3$ under 10 vol% CO_2 atmosphere must be greater than 1000 °C. Therefore, at this low temperature range (900–1030 °C), the reaction involving a decomposition of $SrCO_3$ into SrO and CO_2, and a subsequent SrO reaction with Al_2O_3 are unlikely. Moreover, the intermediate phase, $Sr_3Al_2O_6$, resulting from the direct reaction of $SrCO_3$ and $SrAl_2O_4$ was not observed at this temperature range. Thus, there is another reason to induce $SrCO_3$ decomposition at 900–1030 °C under 10 vol% CO_2 atmosphere. The TEM micrograph (Fig. 2), diffraction patterns and EDS (Fig. 3) results indicate that the Al^{3+} ions may diffuse through the $SrAl_2O_4$ and into $SrCO_3$ lattice to carry out the reaction (Eq. (2)). Therefore, hexagonal $SrCO_3$ formation can be attributed to the diffusion of Al_2O_3, and the formation of $Sr_3Al_2O_6$ is reasonably ascribed to the reaction between $SrCO_3$ and $SrAl_2O_4$.

Using the JMA approach, the kinetic of the first stage weight loss for the $SrCO_3$–Al_2O_3 mixture under 10 vol% CO_2 atmosphere was studied (Fig. 9). The n exponent for this reaction is around 0.5, indicating that it is probably diffusion controlled [19] for the initial interfacial reaction between $SrCO_3$ and Al_2O_3. Through the Arrhenius approach, the weight loss activation energy is about 323.8 kJ/mol.

The last weight loss for the $SrCO_3$ and Al_2O_3 mixture under 10 vol% CO_2 atmosphere takes place at around 1100–1200 °C, which coincides exactly with both the second weight loss stage in the $SrCO_3$ and $SrAl_2O_4$ mixture, and the significant weight loss in pure $SrCO_3$. The activation energies of these weight loss

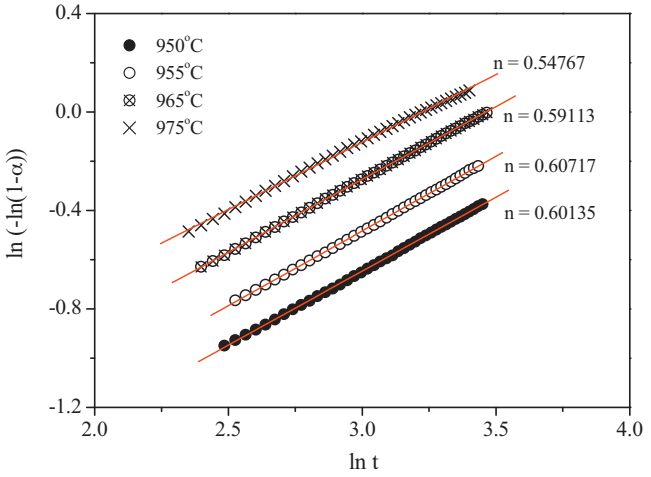

Fig. 9. $\ln(-\ln(1-\alpha))$ vs. $\ln t$ for the 1st-stage weight loss of the $SrCO_3$–Al_2O_3 mixture calcined in 10 vol% CO_2.

stages are 1097.4 kJ/mol, 1060.3 kJ/mol, and 1046.2 kJ/mol, respectively (Fig. 10). Similar activation energy values can be ascribed to the thermal decomposition of pure $SrCO_3$ (Eq. (1)). The n exponents for the admixture with Al_2O_3 and with $SrAl_2O_4$ are both around 0.6–0.8, and the value for the pure $SrCO_3$ is 0.4–0.6. Hancock reported that the decomposition of $BaCO_3$ was controlled by diffusion with an exponent n value close to 0.5 [20]. Therefore, the $SrCO_3$ decomposition occurring around 1100–1200 °C can be considered as a diffusion-controlled mechanism as well and with a leaner development [19]. However, the SrO resulting from the $SrCO_3$ decomposition was not observed. The sample calcined at 1200 °C under 10 vol% CO_2 atmosphere only shows the formation of $SrAl_2O_4$, $Sr_3Al_2O_6$ and remaining Al_2O_3 (Fig. 8). It is supposed that the resulting SrO diffuses rapidly into the product layer. The formation of pure $SrAl_2O_4$ is carried out via a complicated diffusion process at a higher temperature.

Diffusion couple experiments were used to investigate the species diffusion process. The bulks were stacked as shown in Fig. 11. Each couple was heat-treated at 1100 °C for 72 h. For the heat-treated couple stacked like Fig. 11(a), the bottom of $SrAl_2O_4$ bulk shows the formation of new species with different morphology. According to the EDS result (Fig. 12), $Sr_3Al_2O_6$ formation is implied. For the heat-treated couple stacked like Fig. 11(b), the top of the $Sr_3Al_2O_6$ bulk shows the new species formation with various compositions, i.e. the Al/Sr ratio increases from the interior to the top of the bulk (Fig. 13). The species at the most top with Al/Sr ≈ 2 is suggested to be the $SrAl_2O_4$ formation. Nevertheless, SrO formation was not observed in the solid-state reaction between $SrCO_3$ and Al_2O_3. The resulted SrO is supposed to diffuse through the product layer, and take place in the reaction with $Sr_3Al_2O_6$, forming $SrAl_2O_4$. Moreover, Al_2O_3 can diffuse through $SrAl_2O_4$ to react with $Sr_3Al_2O_6$, forming $SrAl_2O_4$. The solid-state reaction should be a dual diffusion mechanism.

The solid-state reaction between $SrCO_3$ and Al_2O_3 under CO_2 atmosphere can be separated into multiple reaction stages.

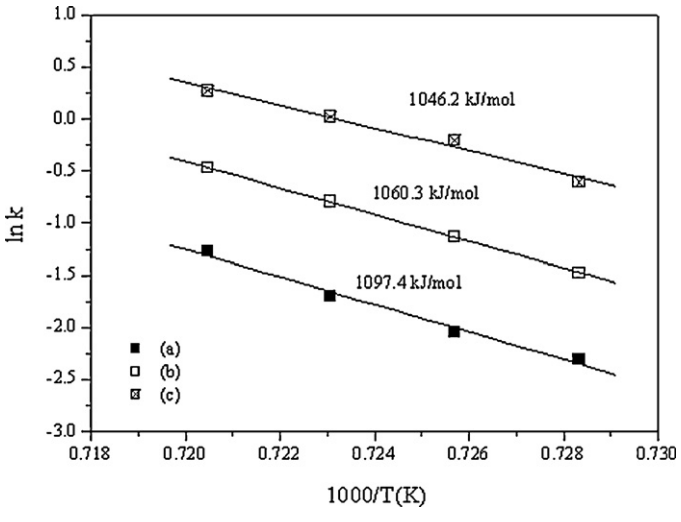

Fig. 10. Arrhenius plots of the third stages of weight loss for the different mixtures, (a) $SrCO_3 + Al_2O_3$, (b) $2SrCO_3 + SrAl_2O_4$, and (c) pure $SrCO_3$.

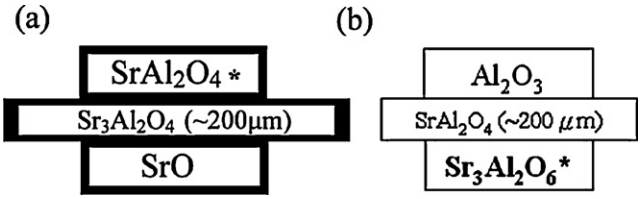

Fig. 11. Stacking scheme for the diffusion couples.

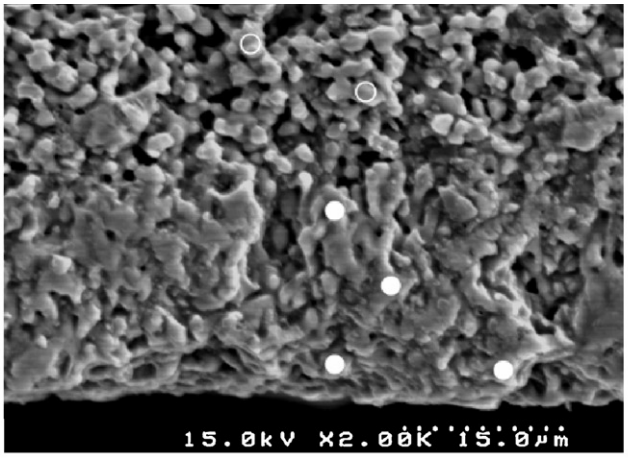

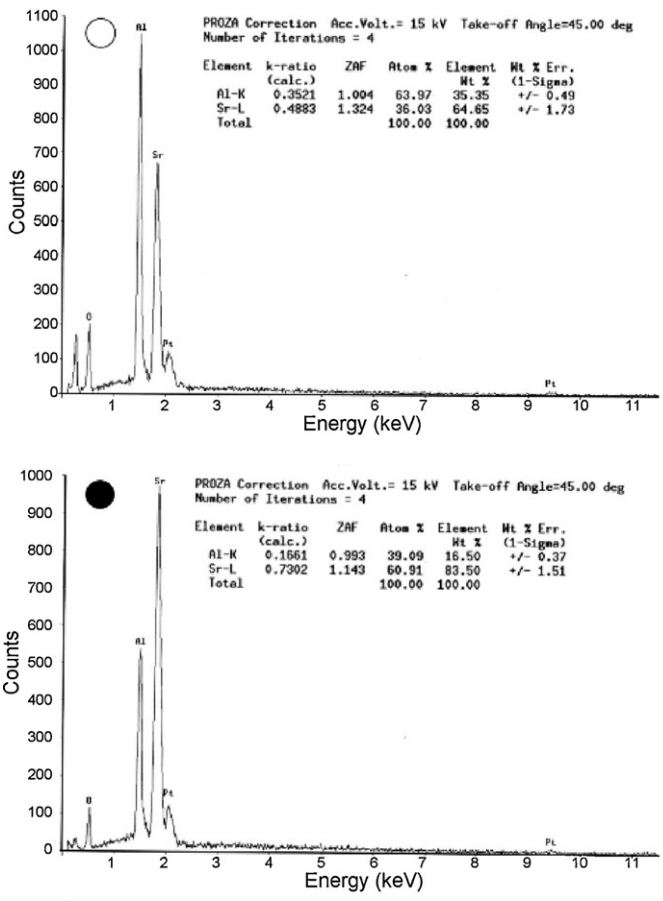

Fig. 12. SEM micrograph and EDS results of the $SrAl_2O_4$ bulk sample.

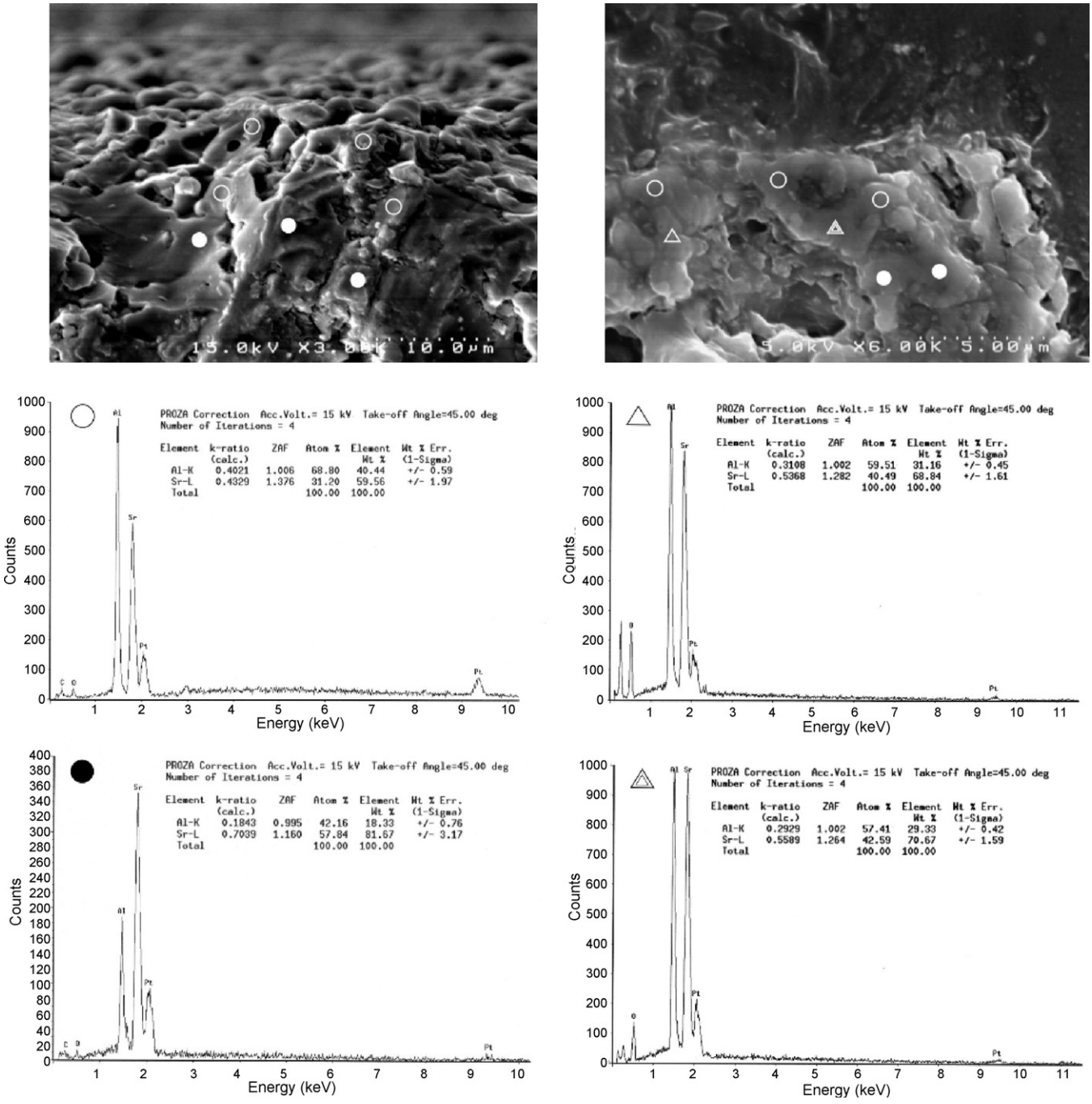

Fig. 13. SEM micrographs and EDS results of the $Sr_3Al_2O_6$ bulk sample.

The reactions are attributed to different diffusion mechanisms. However, these reactions occur at very close temperatures under air atmosphere, which leads to a complex reaction between the solids in air.

4. Conclusions

This study presented the phase evolution of the $SrCO_3$ and Al_2O_3 reaction. The formation of hexagonal $SrCO_3$ and hexagonal $SrAl_2O_4$ was observed under CO_2 atmosphere. The incorporation of excess Al_2O_3 is suggested to stabilize these high-temperature hexagonal species. The estimated lattice parameters of the stabilized hexagonal $SrCO_3$ are $a = 3.99$ Å and $c = 10.49$ Å and the diffraction index was proposed.

The thermal analysis under CO_2 atmosphere was used to investigate the $SrCO_3$ and Al_2O_3 mixture solid-state reaction. The results indicate that the first reaction is attributed to the formation of $SrAl_2O_4$ from the reaction between $SrCO_3$ and Al_2O_3 dominated by Sr^{2+} ion diffusion. The activation energy of the first reaction is about 323.8 kJ/mol. The Al^{3+} ions then diffuse through the product layer to continue the reaction. Subsequently, $Sr_3Al_2O_6$ is formed from $SrCO_3$ and $SrAl_2O_4$ at a higher temperature (900–1030 °C). The $SrCO_3$ thermal decomposition with activation energies of 1046.2–1097.4 kJ/mol finally occurs.

The resulting SrO may diffuse rapidly through the product layer, forming pure $SrAl_2O_4$ via a complicated diffusion process at a higher temperature. These reaction stages occur at very close temperatures under an air atmosphere. The high overlap of these reactions leads to the complex reaction between the solids in air.

Acknowledgment

The authors would like to express their thanks to the Ministry of Economic Affairs of the Republic of China for financially supporting this project (100-EC-17-A-08-S1-170).

References

[1] S.H.M. Poort, W.P. Blokpoel, G. Blasse, Luminescence of Eu^{2+} in barium and strontium aluminate and gallate, Chem. Mater. 7 (1995) 1547.
[2] K.Y. Jung, H.W. Lee, H.K. Jung, Luminescent properties of (Sr, Zn) Al_2O_4:Eu^{2+},B^{3+} particles as a potential green phosphor for UV LEDs, Chem. Mater. 18 (2006) 2249.
[3] T. Katsumata, K. Sasajima, T. Nabae, S. Komuro, T. Morikawa, Characteristics of strontium aluminate crystals used for long-duration phosphors, J. Am. Ceram. Soc. 81 (1998) 413.
[4] V. Singh, T.K.G. Rao, J.J. Zhu, Preparation, luminescence and defect studies of Eu^{2+}-activated strontium hexa-aluminate phosphor prepared via combustion method, J. Solid State Chem. 179 (2006) 2589.
[5] A. Douy, M. Capron, Crystallisation of spray-dried amorphous precursors in the SrO–Al_2O_3 system: a DSC study, J. Eur. Ceram. Soc. 23 (2003) 2075.
[6] Y. Liu, C.N. Xu, Influence of calcining temperature on photoluminescence and triboluminescence of europium-doped strontium aluminate particles prepared by sol–gel process, J. Phys. Chem. B 107 (2003) 3991.
[7] Z. Fu, S. Zhou, S. Zhang, Study on optical properties of rare-earth ions in nanocrystalline monoclinic $SrAl_2O_4$:Ln (Ln = Ce^{3+}, Pr^{3+}, Tb^{3+}), J. Phys. Chem. B 109 (2005) 14396.
[8] D. Ravichandran, S.T. Johnson, S. Erdei, R. Roy, W.B. White, Crystal chemistry and luminescence of the Eu^{2+}-activated alkaline earth aluminate phosphors, Display 19 (1999) 197.
[9] T. Aitasalo, P. Deren, J. Holsa, H. Jungner, J.C. Krupa, M. Lastusaari, J. Legendziewicz, J. Niittykoski, W. Strek, Persistent luminescence phenomena in materials doped with rare earth ions, J. Solid State Chem. 171 (2003) 114.
[10] M.I. Zaki, G.A.M. Hussien, R.B. Fahim, A thermogravimetric study of the solid-state reaction between alumina and strontium carbonate, J. Therm. Anal. 30 (1985) 129.
[11] L.P. Camby, G. Thomas, Kinetic considerations about the successive nucleations of various aluminates in the $BaCO_3$-γ-Al_2O_3 reaction, Solid State Ionics 93 (1997) 315.
[12] M.A. Gulgun, O.O. Popoola, W.M. Kriven, Chemical synthesis and characterization of calcium aluminate powders, J. Am. Ceram. Soc. 77 (1994) 531.
[13] Y.L. Chang, H.I. Hsiang, M.T. Liang, Phase evolution during formation of $SrAl_2O_4$ from $SrCO_3$ and α-Al_2O_3/AlOOH, J. Am. Ceram. Soc. 90 (2007) 2759.
[14] H. Yamada, W.S. Shi, K. Nishikubo, C.N. Xu, Determination of the crystal structure of spherical particles of $SrAl_2O_4$:Eu prepared by the spray method, J. Electrochem. Soc. 150 (2003) E251.
[15] W.S. Shi, H. Yamada, K. Nishikubo, H. Kusaba, C.N. Xu, Novel structural behavior of strontium aluminate doped with europium, J. Electrochem. Soc. 151 (2004) H97.
[16] T. Nishino, Formation process of metastable phase (δ) of alkaline-earth carbonate, J. Am. Ceram. Soc. 70 (1987) C-162.
[17] J.J. Lander, Polymorphism and anion rotational disorder in the alkaline earth carbonates, J. Chem. Phys. 17 (1949) 892.
[18] I. Barin, O. Knacke, Thermodynamical Properties of Inorganic Substances, Springer-Verlag, Berlin, 1973.
[19] C.H. Bamford, C.F.H. Tipper, Comprehensive Chemical Kinetics, Reaction in the Solid State, vol. 22, Elsevier, Oxford, UK/New York, 1980, (ch. 3).
[20] J.D. Hancock, J.H. Sharp, Method of comparing solid-state kinetic data and its application to the decomposition of kaolinite, brucite, and $BaCO_3$, J. Am. Ceram. Soc. 55 (1972) 74.